Magnetism in Graphene Nanoislands

J. Fernández-Rossier[1] and J. J. Palacios[1,2]

[1]*Departamento de Física Aplicada, Universidad de Alicante, San Vicente del Raspeig, Alicante E-03690, Spain*
[2]*Instituto de Ciencia de Materiales de Madrid (CSIC), Cantoblanco, Madrid E-28049, Spain*

(Received 19 July 2007; published 23 October 2007)

We study the magnetic properties of nanometer-sized graphene structures with triangular and hexagonal shapes terminated by zigzag edges. We discuss how the shape of the island, the imbalance in the number of atoms belonging to the two graphene sublattices, the existence of zero-energy states, and the total and local magnetic moment are intimately related. We consider electronic interactions both in a mean-field approximation of the one-orbital Hubbard model and with density functional calculations. Both descriptions yield values for the ground state total spin S consistent with Lieb's theorem for bipartite lattices. Triangles have a finite S for all sizes whereas hexagons have $S = 0$ and develop local moments above a critical size of ≈ 1.5 nm.

DOI: 10.1103/PhysRevLett.99.177204 PACS numbers: 75.75.+a, 73.20.−r, 75.50.Xx, 75.70.Cn

The study of graphene-based field effect devices has opened a new research venue in nanoelectronics [1–5]. Graphene is a truly two-dimensional zero-gap semiconductor with peculiar transport and magnetotransport propreties, including the room temperatrue quantum Hall effect [6], that makes it very different from conventional semiconductors and metals [7]. Progress in the fabrication of graphene-based lower dimensional structures has been reported both in the form of one-dimensional ribbons [8,9] and zero-dimensional dots [2,7,10]. Interestingly, the electronic properties of graphene change in a nontrivial manner when going to lower dimensions. Ribbons, for instance, can be either semiconducting with a size dependent gap or metallic [8,9].

The electronic structure of graphene-based nanostructures is expected to be different from bulk graphene because of surface, or, more properly, edge effects [11]. This is particularly true in the case of structures with zizzag edges which present magnetic properties [12–14]. Whereas bulk graphene is a diamagnetic semimetal, simple tight-binding models predict that one-dimensional ribbons with zigzag edges have two flat bands at the Fermi energy [11,12,15–17], i.e., are paramagnetic metals. Spin polarized density functional theory (DFT) [13] and mean-field [12] calculations confirm that these bands are prone to magnetic instabilities.

The fabrication of graphene nanostructures using top-bottom techniques does not permit creating atomically defined edges to date [10]. In contrast, bottom-up processing of graphene nanoislands is very promising [18]. Hexagonal shape nanoislands with well-defined zigzag edges atop the 0001 surface of Ru have already been achieved [19]. This experimental progress motivates our study of the electronic structure of graphene nanostructures with various shapes. Graphene quantum dots also hold the promise of extremely long spin relaxation and decoherence time because of the very small spin-orbit and hyperfine coupling in carbon [20].

We have found that, remarkably, both the DFT calculations and the mean-field approximation of the single-band Hubbard model with first-neighbors hopping yield very similar results in all cases considered. Our mean-field results are in agreement with the predictions of Lieb's theorem [21] regarding the total spin S of the exact ground state of the Hubbard model in bipartite lattices. The honeycomb lattice of graphene is formed by two triangular interpenetrating sublattices, A and B. Triangular nanostructures have more atoms in one sublattice, $N_A \neq N_B$; our mean-field calculations consistently predict that the total spin of the ground state is $2S = N_A - N_B$ and that is mainly localized on the edges. This could have been anticipated from Hund's rule and the appearance, in the noninteracting model, of $N_A - N_B$ degenerate states with strictly zero energy. Hexagonal nanostructures, for which $N_A = N_B$, result in $S = 0$ ground states even when interactions are turned on. A value of $S = 0$ does not preclude, however, an interesting magnetic behavior. In fact, we predict a quantum phase transition for hexagons: Whereas small ones are paramagnetic, large ones are compensated ferrimagnets, both with $S = 0$.

The shape and the single-particle spectrum.—The different atomic structure of triangular and hexagonal graphene nanostructures can be appreciated in Figs. 1(a) and 1(b). Zigzag edges are formed by atoms that belong to the same sublattice, A or B. In the case of the triangular systems the three edges belong to the same sublattice, hereafter A, whereas in the hexagon three edges are A type and the other three are B type. The edge imbalance in triangular nanostructures results in a global imbalance, so that the total number of atoms in the sublattice A and B is not the same. In what follows we characterize the size of both triangular and hexagonal nanostructures by the integer number N of edge atoms of the same sublattice along one edge of the island (see Fig. 1).

The structural differences between hexagonal and triangular nanostructures reflect in their electronic properties.

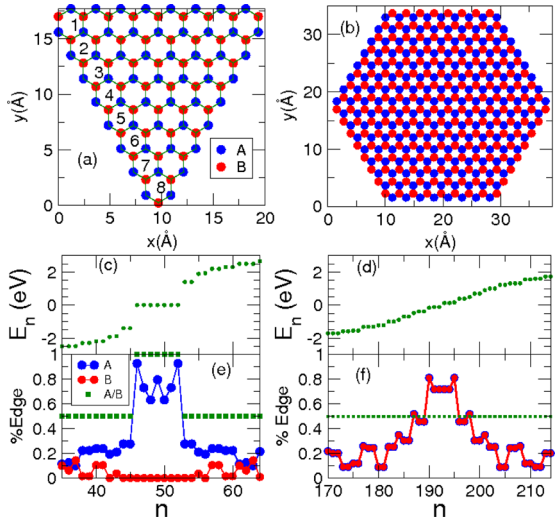

FIG. 1 (color online). (a) and (b) Atomic structure of the triangular and hexagonal graphene islands. (c),(d) Single-particle spectra for the $N = 8$ triangle (left) and hexagon (right). (e),(f) Sublattice resolved edge content and sublattice polarization.

At the simplest level, we describe them in the one-orbital tight-binding approximation [11,12,15–17]. The model Hamiltonian H_0 is totally defined by the positions of the atoms and the first-neighbor hopping parameter t, which we take equal to 2.5 eV. We set the on-site energies for all the carbon atoms equal to zero. We assume that the edge atoms are pasivated, so that there are no dangling bonds. In Figs. 1(c) and 1(d) we show the (low energy) spectra corresponding to a triangle (left) and a hexagon (right) with edge size $N = 8$. If the system is charge neutral the relevant electronic states, corresponding to the highest occupied and lowest unoccupied molecular orbitals (HOMOs and LUMOs) are around $E = 0$. The most striking difference between the spectra of the triangle and the hexagon is the existence of a cluster of zero-energy states in the case of the triangle. A sufficient condition to have N_Z states with strict zero energy in graphene structures is to have a sublattice imbalance $N_Z = N_A - N_B$. In the case of graphene islands with triangle shape (see Fig. 1), the sublattice imbalance satisfies $N_A - N_B = N - 1$.

In order to quantify the edge or bulk character of the single-particle eigenstates $\phi_n(I)$, we define their sublattice resolved edge content $W_\eta(n) = \sum_{I\eta,\text{edge}} |\phi_n(I)|^2$, where $\eta = A$, B and I runs over the N_η atoms. We also define the sublattice polarization $\mathcal{L}(n) = \sum_{IA} |\phi_n(I)|^2 - \sum_{IB} |\phi_n(I)|^2$. Both in the case of the triangle [Fig. 1(e)] and the hexagon [Fig. 1(f)] states have a predominant edge character close to the Dirac point ($E = 0$), but, again, there are some differences. In the triangle, the zero-energy states have a full sublattice polarization $\mathcal{L} = 1$ and their edge content can reach almost 1. In the case of the hexagon there is a perfect AB symmetry ($\mathcal{L} = 0.5$) and the edge content does not go above 0.8.

Electron-electron interactions.—The manifold of $2N_Z$ zero-energy states, including the spin, of the triangle is half filled. Electronic repulsions determine which of the 2^{N_Z} spin configurations has the lowest energy. If Hund's rule operates in this system, the ground state of triangular graphene nanostructures (or any other sublattice unbalanced graphene systems, for that matter) should have a maximal magnetic moment $2S = N_Z$. In contrast, the single-particle spectra of hexagons features some dispersion, which acts against interaction induced spin polarization. To put this on a quantitative basis, we have calculated the electronic structure using both a mean-field decoupling of the one-orbital Hubbard model and DFT calculations in a generalized gradient approximation (GGA) as implemented in the GAUSSIAN03 code [22], using an optimized minimal basis set [23].

In the mean-field approximation for the Hubbard model we solve iteratively the Hamiltonian

$$H = H_0 + U \sum_I n_{I\uparrow} \langle n_{I\downarrow} \rangle + n_{I\downarrow} \langle n_{I\uparrow} \rangle, \tag{1}$$

where H_0 is the single-particle Hamiltonian described above and $\langle n_{I\sigma} \rangle$ is the statistical expectation value of the spin-resolved density on atom I, obtained using the eigenvectors of H. This mean-field decoupling can describe spontaneous symmetry breaking along a chosen axis. The results shown here were obtained fixing $N_\uparrow$ and $N_\downarrow$, with $N_\uparrow + N_\downarrow$ equal to the number of carbon atoms in the structure. This permits comparing with DFT calculations where one typically fixes $N_\uparrow - N_\downarrow$. A self-consistent solution of H is characterized by the spin density $m_I \equiv \frac{n_{I\uparrow} - n_{I\downarrow}}{2}$, and a single-particle spectrum $\epsilon_{n,\sigma}$. The total spin $S = \sum_I m_I$ obviously satisfies $S = \frac{N_\uparrow - N_\downarrow}{2}$.

Uncompensated lattices: Triangles.—In Fig. 2 we show the spectrum and the spin density for a $N = 8$ triangle. Upper panels correspond to DFT results with hydrogen passivation of the edge atoms. The results in the lower panel correspond to the mean-field results for the Hubbard model. In both cases we have verified that the solutions with $N_\uparrow - N_\downarrow = N_Z = 7$ have lower ground state energy than solutions with different value of $2S$. The typical energy differences are above 0.5 eV. We choose the value of U such that the HOMO-LUMO gap in the majority spectrum is the same. In the case shown in Fig. 2 this corresponds to $U = 3.85$ eV. Notice that the mean-field and DFT spectrum have very similar structure in the neighborhood of E_F. Interactions open a spin gap in the single-particle zero-energy manifold, resulting in maximal spin polarization of those states. The magnetization density of both calculations is also very similar: The A atoms on the edge are copolarized positively (right arrows) and their B neighbor atoms are copolarized negatively. The net total spin is mostly sitting on the edge and the local magnetization goes to zero in the center of the island. Using the same procedure as above to fix U, we find that its value decreases as the size of the islands increase. The values of U so

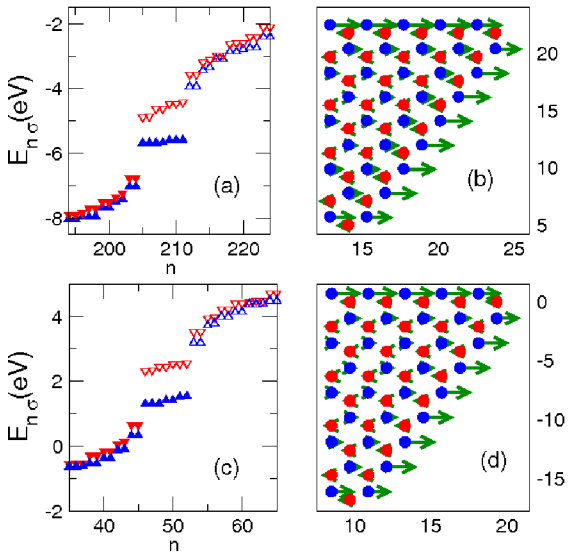

FIG. 2 (color online). Left column: self-consistent energy spectra for a graphene triangular island with $N = 8$ [Fig. 1(a)]. Closed (empty) symbols correspond to full (empty) single-particle states. Right column: local magnetization close to 1 of the corners of the triangle. Upper row: DFT calculations. Lower row: mean-field calculations with the Hubbard model. Magnetization arrows are plotted horizontally for the sake of clarity.

obtained are always below the critical value $U \simeq 2.2t \simeq 5.5$ eV above which infinite graphene would become antiferromagnetic [12,24].

These results indicate that the Hubbard model captures the low-energy physics of graphene triangular nanoislands. One can conclude that next-to-nearest neighbor hopping, long-range Coulomb interactions, and correlations, as included in the DFT calculations, have a minor effect on the low energy sector. Importantly, the basic features of the mean-field solutions, like the structure of the spectrum, the total spin of the ground state and the magnetization density, are very robust with respect to the value of U. We have found very similar results for triangles with N between 5 and 30. The solution that minimizes the ground state energy always satisfies

$$2S = N_\uparrow - N_\downarrow = N_A - N_B = N_Z = N - 1. \qquad (2)$$

Our mean-field Hubbard model and DFT results are in agreement with the Lieb theorem that states that the spin S of the ground state of a Hubbard model in a bipartite lattice satisfies the relation $2S = N_A - N_B$ [21]. If the Hubbard model with first-neighbors hopping and constant U can be applied to graphene-based structures of arbitrary shape, the theorem permits to predict the spin of the ground state by simple counting of the sublattice imbalance. The fact that the number of strict zero-energy states N_Z equals to $N_A - N_B$ provides a simple picture of how the magnetization comes about: Spin polarization results from Hund's rule and the absence of kinetic energy penalty in sublattice unbalanced graphene structures.

Compensated lattices: Hexagons.—In the case of balanced structures Lieb's theorem predicts that they have $S = 0$. This is compatible with a locally unpolarized state, but also with locally polarized solutions with antiferromagnetic correlations. In these cases, calculations are necessary to obtain the local magnetization density. In the case of hexagons there is a competition between the dispersion of the single-particle spectra and interactions. Dispersion occurs because of the hybridization of states that otherwise would lie in a single sublattice close to the edge. These states overlap in the inner region and close to the vertices and hybridize through hopping in H_0. Smaller nanostructures feature larger hybridization and are less prone to develop magnetic order. In the case of hexagons we expect a critical size above which exchange interactions take over and the edges magnetize. This is indeed what we have obtained from our mean-field calculations.

The local magnetization m_I for the $N = 8$ hexagon with $U = 2.5$ eV is shown in the right panel of Fig. 3. The local magnetic moments lie mainly on the edges. We quantify the formation of local moments in compensated structures by the sublattice resolved average magnetic moment on the edge atoms $\langle m_\eta \rangle_{\text{edge}} = \sum_{I\eta}{}' m_I/3N$, where $\eta = A, B$ and the sum runs over the $3N$ edge atoms of the η sublattice in the hexagon. For a given value of U, there is a critical value of N below which this quantity is zero. In Fig. 3(a) we plot $\langle m_\eta \rangle_{\text{edge}}$ as a function of N for three different values of U. We always find that $\langle m_A \rangle_{\text{edge}} = -\langle m_B \rangle_{\text{edge}}$. This panel also shows how the critical size depends on U. When sweeping U in a rather wide range ($U = 1.5$ to $U = 3.5$ eV) the largest possible paramagnetic hexagon goes from 7 to 4. We have also estimated the critical size with the help of DFT calculations and found that the largest paramagnetic

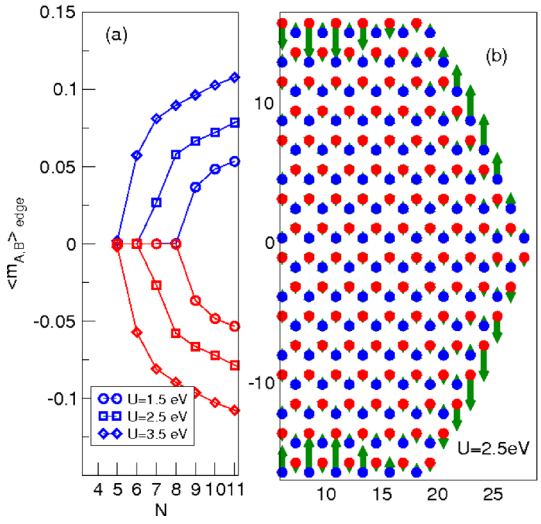

FIG. 3 (color online). (a) Sublattice resolved average magnetic moment as a function of N for 3 values of U. (b) Magnetization density for $U = 2.5$ eV and $N = 8$. Arrows are plotted vertically for the sake of clarity.

hexagon corresponds to $N = 8$, which is consistent with the mean-field Hubbard results for small $U = 1.5$ eV.

Final remarks and conclusions.—We have seen how the magnetic properties of graphene nanostructures are intimately related to the sublattice imbalance $N_A - N_B$ in agreement with Lieb's theorem [21]. This is related to previous work on vacancies in graphene [25]. As a consequence of Lieb's theorem a single vacancy results in the formation of a local moment with $S = 1/2$ and the sign of the spin coupling between two single atom vacancies would depend on whether or not they belong to the same sublattice [26]. The correlation between sublattice and sign of the exchange interaction is also seen in our results for triangular and hexagonal nanoislands: Moments in the same sublattice couple ferromagnetically whereas moments in different sublattices couple antiferromagnetically. Indirect exchange interaction in graphene follows the same rule [27].

Nanomagnets show remanence and hysteresis because of magnetic anisotropy, which originates in the spin-orbit interaction, very small in graphene. Therefore, the *direction* of the spontaneous magnetization, $\vec{M}$, of graphene nanoislands will fluctuate in the absence of an applied magnetic field. At zero field, the detection of magnetism should rely on properties that depend on $|\vec{M}|$, the modulus of the magnetization vector. An example of this is the quasiparticle density of states, as probed with single electron transport in systems with spin polarization and without magnetic anisotropy [28]. The controlled addition of single electrons to other nanomagnetic structures, like magnetic semiconductor quantum dots [29], afford the electrical control of their magnetic properties. This deserves further attention in the case of magnetic graphene nanoislands.

In conclusion, we have studied the emergence of magnetism in graphene nanoislands with well-defined zigzag edges. Our DFT calculations suggest that the magnetic structure of the ground state of graphene nanoislands can be described with a simple Hubbard model. Ground states with finite spin S appear in structures in which the number of atoms of one of the sublattices is larger than the other, $N_A > N_B$, like triangular islands. The single-particle spectrum of these structures features $N_Z = N_A - N_B$ states with strictly zero energy, localized in the A sublattice, which yield a magnetic ground state with finite magnetic moment $S = \frac{N_A - N_B}{2}$ when interactions are included, both in a mean-field Hubbard model and with DFT calculations. Compensated structures ($N_A = N_B$) like hexagons have $S = 0$. However, they develop spontaneous sublattice magnetization above a critical size. All our results are nicely consistent with Lieb's theorem [21] and complement the theorem in the case of $S = 0$ ground states.

We acknowledge useful discussions with F. Guinea, B. Wunch, R. Miranda, and L. Brey. This work has been financially supported by MEC-Spain (Grant No. FIS200402356 and Ramon y Cajal Program), by Generalitat Valenciana (No. Accomp07-054), by Consolider No. CSD2007-0010 and, in part, by FEDER funds.

Note added.—Upon the completion of this work we have been aware of a related work by E. Ezawa [30], in the single-particle approximation, and De-en Jiang *et al.* and O. Hod *et al.* doing DFT calculations [31].

[1] K. S. Novoselov *et al.*, Science **306**, 666 (2004).
[2] J. Scott-Bunch *et al.*, Nano Lett. **5**, 287 (2005).
[3] K. S. Novoselov *et al.*, Nature (London) **438**, 197 (2005).
[4] Y. Zhang *et al.*, Nature (London) **438**, 201 (2005).
[5] C. Berger *et al.*, Science **312**, 1191 (2006).
[6] K. S. Novoselov *et al.*, Science **315**, 1379 (2007).
[7] A. Geim and K. Novoselov, Nat. Mater. **6**, 183 (2007)
[8] Z. Chen *et al.*, arXiv:cond-mat/0701599.
[9] M. Y. Han *et al.*, Phys. Rev. Lett. **98**, 206805 (2007).
[10] B. Ozyilmaz *et al.*, Phys. Rev. Lett. **99**, 166804 (2007).
[11] K. Nakada *et al.*, Phys. Rev. B**54**, 17 954 (1996).
[12] M. Fujita *et al.*, J. Phys. Soc. Jpn. **65**, 1920 (1996).
[13] Young-Woo Son, M. L. Cohen, and S. G. Louie, Nature (London) **444**, 347 (2006); Y.-W. Son, M. L. Cohen, and S. G. Louie, Phys. Rev. Lett. **97**, 216803 (2006); O. Hod *et al.*, Nano Lett. **7**, 2295 (2007).
[14] K. Wakabayashi, M. Sigrist, and M. Fujita, J. Phys. Soc. Jpn. **67**, 2089 (1998).
[15] M. Ezawa, Phys. Rev. B **73**, 045432 (2006).
[16] L. Brey and H. Fertig, Phys. Rev. B**73**, 235411 (2006).
[17] F. Munoz-Rojas *et al.*, Phys. Rev. B **74**, 195417 (2006).
[18] J. Wu, W. Pisula, and K. Mullen, Chem. Rev. **107**, 718 (2007).
[19] A. L. Vázquez de Parga *et al.*, arXiv:0708.0360.
[20] B. Trauzettel *et al.*, Nature Phys. **3**, 192 (2007).
[21] Elliott H. Lieb, Phys. Rev. Lett. **62**, 1201 (1989).
[22] M. J. Frisch *et al.*, GAUSSIAN 03, Rev. B.01 (Gaussian, Inc., Pittsburgh PA, 2003).
[23] M. M. Hurley *et al.*, J. Chem. Phys. **84**, 6840 (1986).
[24] N. Peres, M. A. N. Araujo, and D. Bozi, Phys. Rev. B **70**, 195122 (2004).
[25] M. A. H. Vozmediano *et al.*, Phys. Rev. B **72**, 155121 (2005).
[26] H. Kumazaki and D. S. Hirashima, J. Phys. Soc. Jpn. **76**, 064713 (2007).
[27] S. Saremi, arXiv:0705.0187 [Phys. Rev. B (to be published)]; L. Brey, H. A. Fertig, and S. Das Sarma, Phys. Rev. Lett. **99**, 116802 (2007).
[28] C. Gould *et al.*, Phys. Rev. Lett. **97**, 017202 (2006); J. Fernández-Rossier and R. Aguado, Phys. Rev. Lett. **98**, 106805 (2007).
[29] J. Fernández-Rossier and L. Brey, Phys. Rev. Lett. **93**, 117201 (2004); Y. Leger *et al.*, Phys. Rev. Lett. **97**, 107401 (2006).
[30] M. Ezawa, arXiv:0707.0349.
[31] De-en Jiang, B. G. Sumpter, and S. Dai, arXiv:0706.0863; O. Hod, V. Barone, and G. E: Scuseria, arXiv:0709.0938.